

INTRACLUSTER ENTROPY FROM JOINT X-RAY AND SUNYAEV-ZEL'DOVICH OBSERVATIONS

A. CAVALIERE¹, A. LAPI^{1,2}, AND Y. REPHAELI³

Draft version January 30, 2019

ABSTRACT

The temperature and density of the hot diffuse medium pervading galaxy groups and clusters combine into one significant quantity, the entropy. Here we express the entropy levels and profiles in model-independent forms by joining two observables, the X-ray luminosity and the change in the CMB intensity due to the Sunyaev-Zel'dovich (SZ) effect. Thus we present both global *scaling* relations for the entropy levels from clusters and groups, and a simple expression yielding the entropy *profiles* in individual clusters from resolved X-ray surface brightness and SZ spatial distributions. We propose that our approach provides two useful tools for comparing large data samples with models, in order to probe the processes that govern the thermal state of the hot intracluster medium. The feasibility of using such a diagnostic for the entropy is quantitatively assessed, based on current X-ray and upcoming SZ measurements.

Subject headings: cosmic microwave background - X rays: galaxies: clusters

1. INTRODUCTION

Recent X-ray observations of the hot intracluster medium (ICM) filling galaxy groups and clusters have indicated problems with both the levels of the density, $n \sim 10^{-3} \text{ cm}^{-3}$, and the distribution of the temperature T , with average values $kT \sim 10 - 1/2 \text{ keV}$ from very rich clusters to poor groups. First, the lower densities found in poor clusters and groups imply mass ratios m/M of ICM to dark matter (DM) considerably below the cosmic baryonic fraction approached in rich clusters (see Sanderson & Ponman 2003, Pratt & Arnaud 2003).

Second, radial profiles $T(r)$ have been measured, if coarsely, in several nearby clusters; they show a roughly isothermal plateau extending out to substantial radii $r \approx 0.1 - 0.2R$ in terms of the virial radius R , and then a decline by a factor 1/2 out to $R/2$ (Markevitch et al. 1998, De Grandi & Molendi 2002, Vikhlinin et al. 2005). Although still debated in detail, this behavior differs from the predictions of simple modeling in terms of a polytropic equation of state $T(r) \propto n^{\Gamma-1}$ with constant index $1 \leq \Gamma \leq 5/3$. It also differs at $r \lesssim 0.2R$ from the outcomes of most state-of-the-art numerical simulations, where $T(r)$ keeps rising toward the cluster center to $r \sim 0.05R$ as discussed, e.g., by Borgani et al. (2004). A central, limited dip of $T(r)$ observed in many clusters (e.g., Piffaretti et al. 2005) and often referred to as a “cool core” (Molendi & Pizzolato 2001) is arguably attributed to a quenched “cooling flow” (see the discussion by Fabian 2004). Such dips involve ICM fractions of some 10^{-3} and constitute a specific issue not of direct concern here.

To focus the problems in the *bulk* of the ICM, temperature and density are conveniently combined into a significant single quantity, the specific entropy \mathfrak{s} ; here we adopt the widely used adiabat $K \equiv kT n^{-2/3}$, which is related to \mathfrak{s} by $K \propto e^{2\mathfrak{s}/3k}$ (Bower 1997; Balogh, Babul & Patton 1999). The quantity K constitutes the simplest combination of n and T that is invariant under adiabatic processes in the ICM; nonadiabatic processes compete to produce different levels and profiles of

K , that cooling always lowers and various heating processes tend to raise.

When the data on n and T are combined to yield K , it is found that (i) in moving from clusters to groups the *levels* of K decline only slowly (in fact, like $K \propto T^{2/3}$) taking on values from around 10^3 to some 10^2 keV cm^2 ; (ii) in clusters the entropy *profiles* $K(r)$ have to be described in terms of a running index

$$\Gamma(r) \equiv \frac{5}{3} + \frac{d \ln K}{d \ln n}, \quad (1)$$

that implies profiles $K(r)$ flattening inwards.

These findings may be unified under the heading of an entropy “*excess*” in the ICM. The baseline is provided by gravitational heating, the basic process that affects the thermal state of the ICM during its inflow into the structures as they are built up by standard hierarchical clustering (Peebles 1993). During the buildup, the DM component sets the gravitational potential wells into which the baryons fall, starting with the cosmic density ratio close to 0.16 (Bennett et al. 2003). If the baryons start cold, they fall in supersonically, and are shock-heated to temperatures T close to the virial value T_V (Cavaliere, Menci & Tozzi 1999; Tozzi & Norman 2001; Voit et al. 2003). However, such a process produces (see Ponman, Sanderson, & Finoguenov 2003): (i) entropy levels lower than observed in groups and poor clusters; (ii) entropy profiles in rich clusters that decline too steeply inwards, in fact, as $K(r) \propto r^{1.1}$.

Such drawbacks have raised a wide debate concerning the nature of the additional processes that increase the entropy of the ICM; suggestions include the following possibilities. Energy drain by radiative cooling extended well beyond the very central cool core may cause much of the cold gas to condense into stars, leaving a residual diffuse component with higher entropy (Voit & Bryan 2001); however, such a cooling alone would produce too much cold gas and too many stars (e.g., McCarthy et al. 2004). Repeated energy inputs by supernovae and active galactic nuclei preheat the gas external to forming groups or clusters, raise its state to a higher adiabat, and are expected to hinder its inflow under any model (Evrard & Henry 1991; Kaiser 1991); specifically, as the inflow becomes less supersonic, the shocks are weakened while additional entropy is carried in (Valageas & Silk 1999; Wu,

¹ Dip. Fisica, Università Tor Vergata, via Ricerca Scientifica 1, I-00133 Roma, Italy

² Astrophysics Sector, SISSA/ISAS, Via Beirut 2-4, I-34014 Trieste, Italy

³ School of Physics and Astronomy, Tel Aviv University, 69978 Tel Aviv, Israel

Fabian & Nulsen 2000; Cavaliere, Lapi & Menci 2002a). Energy impulsively discharged by powerful quasars into their ambient medium propagates outwards beyond the host galaxy into a surrounding group (Mazzotta et al. 2004a; McNamara et al. 2005); the propagation may occur in the form of outgoing, moderately supersonic blast waves which at the leading shocks raise the entropy in the gas they sweep up (Lapi, Cavaliere & Menci 2005). Finally, in rich clusters thermal or turbulent diffusion may be effective in depositing and/or smearing out entropy inward of $r \approx R$ (Narayan & Medvedev 2001; Kim & Narayan 2003; Lapi & Cavaliere, in preparation).

Pinning down the leading process clearly requires precise measurements of the levels and profiles of the all-important adiabat K . The state variables n and T that determine K may be measured with X-ray observations (see Sarazin 1988). The bolometric bremsstrahlung emissions $L_X \propto n^2 \sqrt{T} R^3 \approx 10^{42} - 10^{45} \text{ erg s}^{-1}$ primarily provides n , while spatially resolved spectroscopy (continuum plus emission lines) can yield the temperatures T when enough photons are collected.

On the other hand, the hot ICM electrons inverse-Compton scatter the CMB photons crossing a cluster; this Sunyaev-Zel'dovich effect (SZ, Sunyaev & Zel'dovich 1972) constitutes a major ICM (and cosmological) probe in the μ wave and submm bands, as reviewed by Rephaeli (1995), Birkinshaw (1999), and Carlstrom, Holder & Reese (2002). The intensity of the thermal SZ effect is given by the Comptonization parameter $y \propto nTR$, which constitutes a good measure of the electron pressure $p \propto nT$ in the ICM; so far it has been observed in many rich clusters at the expected levels $y \approx 10^{-4}$ (Zhang & Wu 2000; Grainge et al. 2002; Reese et al. 2002; Benson et al. 2004). The main dependencies of $L_X \propto n^2$ and $y \propto p$ strongly motivate us to employ the results of X-ray and SZ observations combined as to provide the adiabat in the form $K \propto pn^{-5/3}$, in order to better probe properties of, and processes in the ICM.

2. SCALING THE ENTROPY LEVELS FROM CLUSTERS TO GROUPS

The levels $K_{0.1}$ of the entropy (usually sampled at $r \approx 0.1 R_{200} \approx 0.08 R$, see Ponman et al. 2003) and of the X-ray luminosity L_X (dominated by the inner ICM anyway) are linked by the relation

$$K_{0.1}/K_g \propto (L_X/L_g)^{-1/3} (T/T_V)^{7/6}, \quad (2)$$

derived in Appendix A. In moving from clusters to groups, this highlights the deviations from the quantities $K_g \propto H^{-4/3} T_V$ and $L_g \propto HT_V^2$ that provide the baseline scaling – including the Hubble parameter $H(z)$ – set by the pure gravitational heating (see § 1); the latter implies $T \approx T_V$, and baryon densities simply proportional to those of the DM (Kaiser 1986).

Eq. (2) has been first proposed by Cavaliere, Lapi & Menci (2002b); similar expressions have been subsequently used by Dos Santos & Dorè (2002), and McCarthy et al. (2003), in the context of specific models for entropy enhancement. Here we stress the *model-independent* nature of Eq. (2); the latter holds whenever the ICM fills in a statistical, virial-type equilibrium a DM potential well, and depends weakly on specific DM distributions or specific equations of state for the ICM. This is demonstrated in Appendix A and Table A1, where we show that from clusters to groups the prefactor on the r.h.s. of Eq. (2) depends weakly on T , so as to closely preserve the above scaling.

We illustrate the role that Eq. (2) may play in probing the processes that set the ICM thermal state. We first recall that in poor clusters and groups with kT ranging from about 4 to about 1/2 keV the observed values of L_X are found to be progressively lower than L_g by factors from 10^{-1} to 10^{-3} , with a steep decline close to $L_X \propto T^3$ (Osmond & Ponman 2004). In other words, moving toward smaller and cooler structures the ICM is found to be progressively underluminous, hence *underdense* relative to the gravitational values. The outcome is even more surprising on two accounts: smaller structures ought to have condensed earlier from a denser Universe; moreover, emission lines from highly excited metals add to the bremsstrahlung continuum to yield a flatter gravitational scaling $L_X \approx L_g \propto T$ for $kT < 2$ keV (see Appendix A). According to Eq. (2), the systematically *lower* values of L_X/L_g will correspond to *higher* entropy levels, exceeding K_g by factors up to 10. In detail, the steep relation $L_X \propto T^3$ will reflect into a flat behavior $K_{0.1} \propto T^{2/3}$, which indeed agrees with recent data analyses (see Ponman et al. 2003).

On the other hand, a number of authors (e.g., Mahdavi et al. 1997; Roussel, Sadat & Blanchard 2000) have questioned the significance of the data concerning groups, given various observational and systematic uncertainties related to the limited statistics and to the necessary subtraction of considerable contributions from single galaxies. Recent critical assessments of the data (Mushotzky 2004; Osmond & Ponman 2004) acknowledge the relevance of these problems in individual groups, but confirm the general trend toward lower densities in poorer systems, albeit with a wide scatter.

To cross-check these low X-ray luminosities L_X , one may preliminarily use the SZ effect; in fact, these two independent probes of the ICM density are expected to correlate according to

$$y_0/y_g \propto (L_X/L_g)^{1/2} (T/T_V)^{3/4}. \quad (3)$$

Here y_0 is the Comptonization parameter integrated along a “central” line of sight (l.o.s.), and $y_g \propto HT_V^{3/2}$ gives its gravitational scaling after Cole & Kaiser (1988); see Appendix A for the derivation and added detail, including a discussion of the contributions to y_0 from the outer ICM. When $L_X \propto T^3$ applies, Eq. (3) predicts the scaling $y_0 \propto T^2$ to hold in equilibrium conditions (Cavaliere & Menci 2001). Such systematically lower values of $y_0/y_g \propto T^{1/2}$ may be tested or bounded with high-sensitivity SZ observations of poor clusters and groups, as initiated by Benson et al. (2004).

Then one can proceed to directly obtain the entropy levels from the equilibrium relations Eqs. (2) and (3). Upcoming SZ measurements will provide high-sensitivity data, which will be conveniently joined with X-ray fluxes to obtain entropy levels that scale as

$$K_{0.1} \propto H^{-8/3} y_0^{10/3} L_X^{-2}, \quad (4)$$

in equilibrium conditions but otherwise in a model-independent way. In moving to groups where line emission is important, Eq. (4) goes over to $K_{0.1} \propto H^{-5/3} y_0^{4/3} L_X^{-1}$; Appendix A gives the details, including the slow dependence on T of the prefactor. Note that the present approach bypasses two difficulties (discussed, e.g., by Mazzotta et al. 2004b) in deriving the ICM temperatures from spatially resolved X-ray spectroscopy: (i) the latter requires more photons than imaging, so with comparable observation times and efficiencies, precise T are obtained at smaller radii than n ; ii) in a multi-phase medium spectroscopic determinations of T are biased toward the colder regions.

The integrated SZ flux $Y \propto y_0 R^2 / d_A^2$, where $d_A(z)$ is the angular diameter distance, may be used instead of the central parameter y_0 ; in terms of Y , Eq. (4) may be recast as

$$K_{0.1} \propto d_A^{20/9} H^{2/3} Y^{10/9} L_X^{-8/9}. \quad (5)$$

Using this relation has two advantages over Eq. (4). Not only is Y a more robust observable in clusters with a cool core (e.g., Benson et al. 2004), but also $Y \propto n T R^3$ has the same R^3 dependence as L_X . So the combination is largely free of the size effects due to the scaling $R \propto T^{1/2}$ for coeval structures (cf. Eq. [A2]); it rather highlights the dependence on the baryonic fraction.

So far we have dealt with the overall entropy *levels* determined from the integrated X-ray and SZ observables. But the entropy *profiles* of individual clusters carry additional information; clearly this will be difficult to extract from the prefactors in global relations like Eqs. (2)-(5), encased as it is under integrated forms within ratios or products of shape factors, as made explicit in Appendix A.

3. RESOLVING THE ENTROPY PROFILES IN CLUSTERS

To go beyond the above global scaling laws, spatially resolved X-ray and SZ observations are clearly required. In X rays, *Chandra* and *XMM-Newton* are already providing data at a few arcsec resolutions; but obtaining both the good spatial and *spectral* resolution needed to measure $T(r)$ and derive $K(r)$ still presents a challenge, especially in the outer ICM of distant clusters. Improvements will again be provided by joining measurements of X-ray brightness and of SZ effect with comparable levels of spatial resolutions.

In fact, the prospective good resolution and high sensitivity (added to multi-frequency capabilities) of the many upcoming SZ experiments (for a recent review, see Birkinshaw 2004) stimulate renewed impetus for considering the deprojected quantities that have been discussed from time to time (e.g., Silk & White 1978, Cavaliere 1980).

Here our specific proposal is to use joint X-ray and SZ measurements to derive directly from the data the radial entropy profiles $K(r)$ in the ICM. We will work in terms of the X-ray surface brightness and of SZ intensity distributions, integrated along a l.o.s at a projected distance s from the cluster center. For spherically averaged ICM distributions these observables are related to the corresponding volume quantities by

$$\ell_X(s) = \frac{\Lambda_0}{2\pi(1+z)^4} \int_s^R dr \frac{r}{\sqrt{r^2-s^2}} n^2(r) \sqrt{T(r)} \quad (6)$$

$$y(s) = \frac{2k\sigma_T}{m_e c^2} \int_s^R dr \frac{r}{\sqrt{r^2-s^2}} n(r) T(r),$$

where the constants are defined after Eq. (A1). Note how strongly the X-ray surface brightness decreases as the redshift z increases, while the SZ effect is z -independent, apart from the dilution effect related to the size of the instrumental beam.

To construct the adiabat $K = kT n^{-2/3}$ we need to retrieve the volume quantities $n(r)$ and $T(r)$ from the projected quantities $\ell_X(s)$ and $y(s)$ given by Eqs. (6). Actually, the latter are in the form of two Abel integral equations, which may be solved for the volume quantities along the lines recalled in Appendix B; the results come to

$$n^2 \sqrt{kT} = \frac{4k^{1/2}(1+z)^4}{\Lambda_0} \frac{1}{r} \frac{d}{dr} \int_R^r ds \frac{s}{\sqrt{s^2-r^2}} \ell_X(s) \equiv \mathcal{L}_X(r) \quad (7)$$

$$nkT = \frac{m_e c^2}{\pi \sigma_T} \frac{1}{r} \frac{d}{dr} \int_R^r ds \frac{s}{\sqrt{s^2-r^2}} y(s) \equiv \mathcal{Y}(r).$$

We stress that the two volume quantities $\mathcal{L}_X(r)$ and $\mathcal{Y}(r)$ are defined directly in terms of the observed surface or l.o.s. observables $\ell_X(s)$ or $y(s)$.

Eqs. (7) are easily combined (over the spatial range common to both data sets) to yield the entropy profile in the simple, *model-independent* form

$$K(r) = \mathcal{Y}^{14/9}(r) \mathcal{L}_X^{-10/9}(r). \quad (8)$$

So far we have not assumed any specific equation of state for the ICM, rather we derive it from $K(r)$ above; in particular, the local polytropic index defined in Eq. (1) reads

$$\Gamma(r) = 3 \left[2 \frac{d \ln \mathcal{L}_X}{d \ln \mathcal{Y}} - 1 \right]^{-1}. \quad (9)$$

To illustrate the importance of the profile $K(r)$ we contrast two physical conditions. On the one hand, a reference baseline is provided once again by the gravitational heating associated with smooth accretion of successive shells (involving DM plus gas, as started by Bertschinger 1985) during the hierarchical buildup of a rich cluster. This “surface” process taking place at the outskirts of the growing structure yields $K(r) \propto r^{1.1}$ and $\Gamma \approx 1.1$ in the region $r \approx R$ (Tozzi & Norman 2001). On the other hand, the actual inflow is likely to include additional “volume” processes induced by infall and sinking of lumps, the well-known merging component in the process of structure formation (see Norman 2005). These dynamical events can drive subsonic turbulent diffusion and related entropy transport from the outskirts toward the inner regions (see Goldman & Rephaeli 1991; Ricker & Sarazin 2001; Inogamov & Sunyaev 2003); clearly these processes will enforce entropy profiles flatter than $K(r) \propto r^{1.1}$, a matter expanded upon elsewhere (Lapi & Cavaliere, in preparation). So it is seen that the entropy profiles can help unveiling the actual physical conditions in clusters.

Note that Eqs. (7) also yield the density and temperature profiles in the form

$$n(r) = \mathcal{L}_X^{2/3}(r) \mathcal{Y}^{-1/3}(r) \quad kT(r) = \mathcal{Y}^{4/3}(r) \mathcal{L}_X^{-2/3}(r). \quad (10)$$

Correspondingly, the local cooling timescale for bremsstrahlung emission reads

$$t_c(r) = \frac{3k^{1/2}}{\Lambda_0} \frac{\mathcal{Y}(r)}{\mathcal{L}_X(r)}. \quad (11)$$

Comparing this to the Hubble time provides a criterion to avoid the inclusion of a region like a cool core, where the physical conditions are very different from the rest of the cluster.

So far, our derivations have been free of specific assumptions concerning models for the DM gravitational potentials, or hydrostatic equilibrium, or equation of state. Assuming now detailed hydrostatic equilibrium, one can use the ICM quantities to trace the DM mass distribution (e.g., Bahcall & Sarazin 1977; Fabricant & Gorenstein 1983), and obtain the result

$$M(< r) = \frac{3}{4G\mu m_p} \frac{r^2}{\mathcal{L}_X^{2/3}(r)} \frac{d}{dr} \mathcal{Y}^{4/3}(r); \quad (12)$$

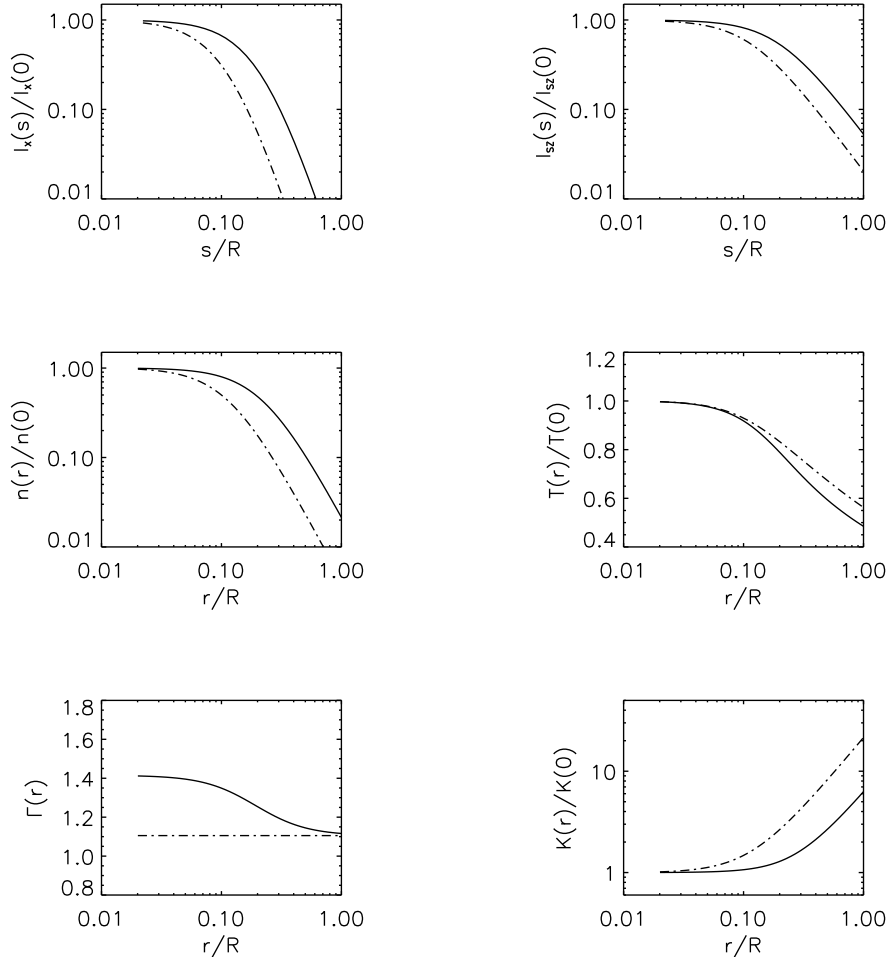


FIG. 1.—Input profiles for the mock experiments described in § 4: X-ray surface brightness, SZ intensity distribution, and radial profiles of density, temperature, entropy and polytropic index. *Dot-dashed* lines are for the simple polytropic model \mathcal{A} with $\Gamma = 1.1$, while *solid* lines are for the nonpolytropic model \mathcal{B} with running index $\Gamma(r)$; see main text for details.

here $\mu \approx 0.6$ is the mean molecular weight for a plasma of one-third solar metallicity, m_p is the proton mass and G is the gravitational constant. Equivalently, Eq. (12) may be used to derive a model for the DM gravitational potential, to be compared with specific forms such as King’s (1972) and NFW (Navarro, Frenk & White 1997), or with the data obtained from gravitational lensing (e.g., Lombardi et al. 2005).

4. MOCK EXPERIMENTS

Given that the imaging capabilities of the present X-ray instruments (*Chandra* and *XMM-Newton*) have attained resolutions down to about $1''$ and fractional sensitivities of order 10^{-3} or better, what can be learned right now by joining these X-ray data with the current, considerably coarser SZ observations?

In fact, here problems arise even for the global scaling laws, and more for profile reconstructions. As discussed in detail by Diaferio et al. (2005), considerable discrepancies as to the scaling laws are found among current SZ samples produced with different instruments, even when the samples have many sources in common. On the other hand, to effectively constrain a fit to the observed SZ distributions often it has been

found necessary to use also X-ray information (see Reese et al. 2003, Benson et al. 2004); this breaks the independence of these two observables that is important for deriving $K(r)$.

A step forward has recently been taken by the observations of the X-ray cluster RX J1347-1145 with the Nobeyama telescope (Komatsu et al. 2001); the good resolution of order $15''$ obtained in these measurements enabled deriving a truly independent SZ profile. In analyzing these data Kitayama et al. (2004) excise the most asymmetric sector, and spherically average the rest to deconvolve the temperature profile, finding results consistent with - but still no better than - the X-ray spectroscopy.

In the light of upcoming SZ capabilities of sub-arcmin resolution and sensitivities better than $10 \mu\text{K}$, we consider next the prospects from measurements with instruments or experiments such as SZA (Holder et al. 2000), AMI (Jones 2002), AMiBA (Lo 2002), MITO (Lamagna et al. 2005), OLIMPO (Masi et al. 2003), ACT (Kosowsky 2003), SPT (Carlstrom et al. 2003), APEX-SZ (Schwan et al. 2003), CARMA (Woody et al. 2004). It is expected that many hundreds of clusters and groups will be detected in a survey mode, with pointed observations of many clusters to sensitivity lev-

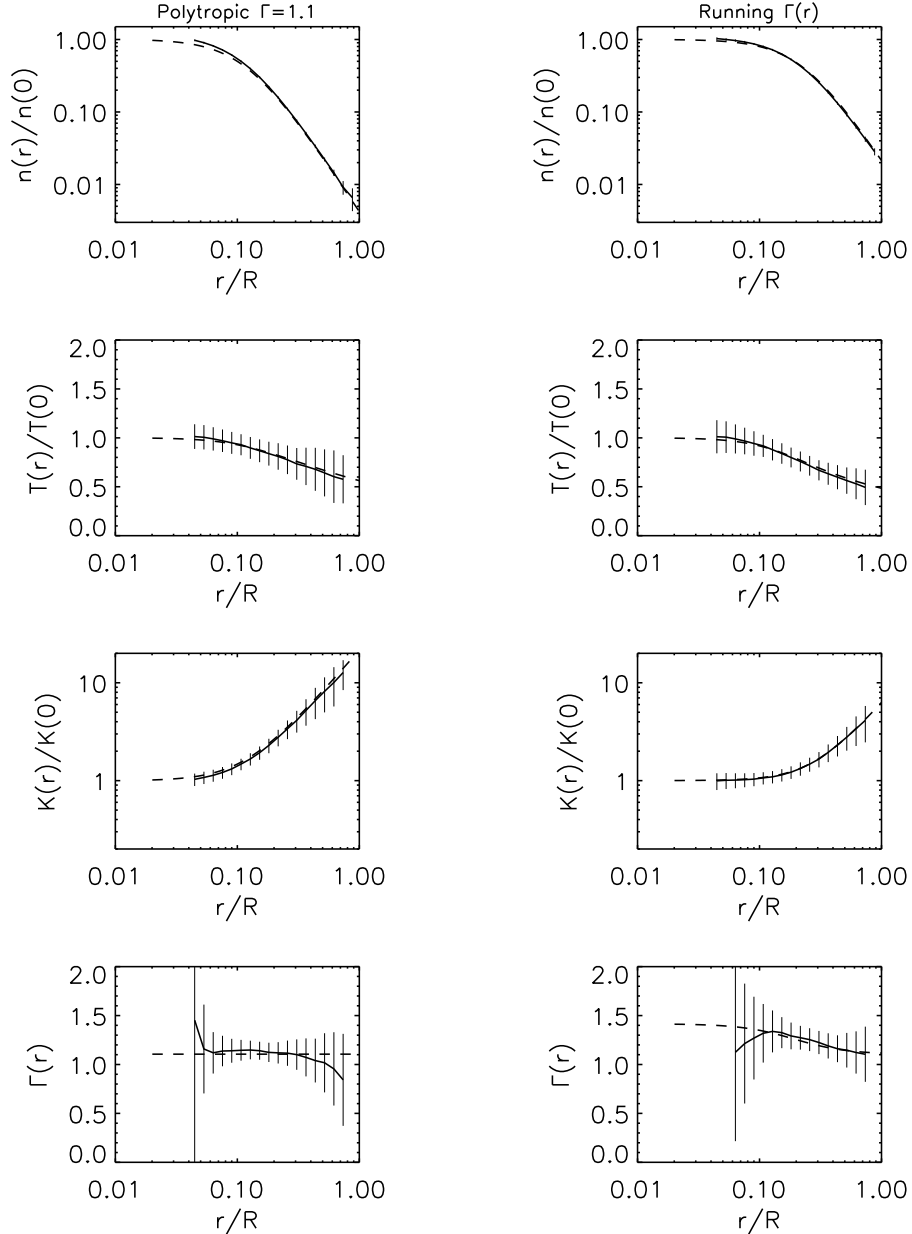


FIG. 2.— Reconstructed profiles from the mock experiments of § 4: radial profiles of density, temperature, entropy, and polytropic index are shown from top to bottom as *solid* lines, with 1σ error bars; *dashed* lines show the input profiles. *Left* column refers to model *A* and *right* column to model *B*.

els of $10\mu\text{K}$ or better. In preselected areas, resolutions down to a few arcsecs will be eventually provided by ALMA (see <http://www.alma.nrao.edu/>), at frequencies on both sides of 220 GHz, the crossover point where the thermal SZ effect goes from negative to positive.

We build mock renditions of the prospective observations as described next. We make use of two *independent*, flexible parameterizations for the spatial distributions of the X-ray brightness and SZ effect; both are of the form

$$I(s) = I(0) \left[1 + \left(\frac{s}{a} \right)^2 \right]^{-b} \quad (13)$$

often adopted for either one, though best suited to clusters with no cool core. Here a is the inner, characteristic radius and b is the shape parameter for the outer profile (e.g., Reese

et al. 2002; Schmidt, Allen & Fabian 2004). Note that a/\sqrt{b} provides an effective “core radius”, while $I(s) \propto s^{-2b}$ approximately holds for large r . To preserve the independence of the two fits, we allow for *different* values of the parameters a_X, a_{SZ} and b_X, b_{SZ} in Eq. (13); note that the isothermal β -model (Cavaliere & Fusco-Femiano 1976; Jones & Forman 1984) would obtain as the particular case where $a_X = a_{SZ}$, $b_X = 3\beta - 1/2 \approx 1.5$ and $b_{SZ} = (3\beta - 1)/2 \approx 0.5$ apply.

First, let us disregard the limitations due to finite resolution and precision; then the fitting formulae Eq. (13) are easily Abel-inverted, and lead to sharp volume distributions $n^2 T^{1/2} \propto [1 + (r/a_X)^2]^{-b_X - 1/2}$ and $nT \propto [1 + (r/a_{SZ})^2]^{-b_{SZ} - 1/2}$ for the X-ray emissivity and SZ effect, respectively. Using

these in Eqs. (8) and (9), the entropy profile reads

$$K(r)/K(0) = \left[1 + (r/a_X)^2\right]^{5(1+2b_X)/9} \left[1 + (r/a_{SZ})^2\right]^{-7(1+2b_{SZ})/9}, \quad (14)$$

while the polytropic index is given by

$$\Gamma(r) = 3 \left[\frac{2+4b_X}{1+2b_{SZ}} \frac{r^2+a_{SZ}^2}{r^2+a_X^2} - 1 \right]^{-1}. \quad (15)$$

These runs are plotted in Fig. 1 for the specific parameter values given in the caption. Note that, when $a_X = a_{SZ}$ is set, a constant value of $\Gamma = (3+6b_{SZ})/(4b_X-2b_{SZ}+1)$ would obtain. Then the bounds $(2b_X-1)/4 \leq b_{SZ} \leq (5b_X-1)/7$ apply; the upper limit corresponds to $\Gamma = 5/3$, i.e., the isentropic profile, while the lower limit corresponds to $\Gamma = 1$, i.e., the isothermal profile.

Next we proceed to generate and analyze mock SZ experiments on introducing prospective resolutions and precisions. We focus on two input models: *A*) a simple polytropic model with constant index $\Gamma \approx 1.1$, which corresponds to Eq. (13) with $b_X = 2.1$, $b_{SZ} = 0.9$, $a_X/\sqrt{b_X} = 0.08R$ and $a_X = a_{SZ}$; *B*) a nonpolytropic model based on Eq. (13) with $b_X = 2.1$, $b_{SZ} = 0.9$, $a_X/\sqrt{b_X} = 0.15R$ and $a_{SZ}/\sqrt{b_{SZ}} = 0.21R$, implying a running index $\Gamma(r)$. These input profiles are illustrated in Fig. 1.

Having in mind rich clusters at $z \lesssim 0.1$, we bin the data into logarithmically equal intervals limited by a central resolution of $10''$; higher resolution, such as eventually attainable with ALMA, will extend the limiting z beyond 0.5. Following Yoshikawa & Suto (1999; see also Tsutsumi et al. 2005, in preparation), we assign 1σ uncertainties $\Delta I_X \approx 2 \times 10^{-4} I_X(0)$ and $\Delta I_{SZ} \approx 10^{-2} I_{SZ}(0)$ to the input X-ray surface brightness and SZ intensity distributions, respectively. Using a standard Monte Carlo scheme we randomly sample Gaussian-distributed values for I_X and I_{SZ} , then perform the reconstruction, and finally average over 1000 realizations.

Fig. 2 shows for each model *A* and *B* the input (*dashed* lines) and reconstructed profiles (*solid* lines with 1σ error bars) of the ICM density $n(r)$, temperature $T(r)$, entropy $K(r)$ and polytropic index $\Gamma(r)$.

It is seen that the average reconstructed profiles are quite similar to the input profiles over a considerable range, in spite of uncertainties and of some systematic deviations increasingly induced at small and large radii by our emulated resolution and sensitivity. It is also seen that the uncertainties in $T(r)$, dominated by the assumed limitations of the SZ observations, considerably exceed those in $n(r)$, mainly contributed by the X-ray observations. On the other hand, the former do not grow fast toward the dimmer outskirts, unlike the X-ray observations particularly of distant clusters in the presence of instrumental or astrophysical background. We add that uncertainties and deviations reduce to about one half when we assume levels of sensitivity and of spatial resolution twice higher than the values used in Fig. 2.

5. DISCUSSION AND CONCLUSIONS

To make optimal use of the precise and resolved, upcoming SZ data we have proposed a simple formalism, which is

model-independent even though formulated here for spherically *averaged* symmetry. Different geometries may be considered along the lines discussed by Binney & Strimpe (1978), and advanced by Zaroubi et al. (2001).

We propose that SZ and X-ray measurements jointly provide useful diagnostic tools aimed at assessing the thermal state of the ICM with the use of large data sets. Specifically, Eqs. (4) or (5) provide simple, global scaling laws for the *levels* of the central entropy $K_{0,1}$ from clusters to groups; on the other hand, in relatively nearby rich clusters Eqs. (8) and (9) directly yield the resolved *profiles* $K(r)$ and the running polytropic index $\Gamma(r)$. The former relations will provide insight on the processes governing the overall thermal state of the ICM in clusters and in groups. The latter relations will probe, e.g., the effectiveness of thermal or turbulent diffusion in establishing the local equation of state for the ICM within rich clusters.

We stress that the scaling in Eq. (3) yields what actually represents a lower limit to y_0 , valid for the ICM in equilibrium within the potential wells. As shown in Table A1 and commented below it in Appendix A, the contribution to y_0 from the outer range $r \gtrsim 0.2R$ is limited to 10–15%, and encased in the shape factors; their slow dependence on system temperature can only yield moderate deviations when the outer and inner regions are described by the same monotonically decreasing hydrostatic distribution. By the same token, upward deviations of y_0 will strongly indicate contributions from outer nonequilibrium plasma, overpressured and outflowing from the wells, an issue that discussions with P. Mazzotta stimulated us to stress. In fact, Lapi, Cavaliere & De Zotti (2003, see their Fig. 3) have computed the transient upper limits expected in 5–10% early bright galaxies and surrounding groups when powerful quasars flare up and drive outgoing blast waves that sweep out part of the ambient medium while raising its pressure and entropy.

In summary, SZ observations with sensitivities of $10\mu\text{K}$ or better and sub-arcmin resolutions will provide the means to scale entropy *levels* in poor clusters and groups out to $z \approx 1.5$. Resolutions of order $10''$ will yield pressure and entropy *profiles*, most valuable in the outskirts of relatively nearby clusters as long advocated by Rephaeli (e.g., 2005). Higher resolutions of a few arcsecs will enable reconstructing the entropy profiles in rich clusters toward $z \approx 1$, where SZ may effectively compete with X rays being unaffected by cosmological dimming. These SZ effect frontiers will afford unprecedented insight on the astrophysics of the ICM.

We thank our referee for several helpful comments and suggestions. We are indebted to P. Mazzotta for critical reading of an earlier version of this paper, and for insightful discussions of the X-ray and SZ differential sensitivities. Work supported by grants from INAF and MIUR at the University of Rome Tor Vergata, and from the Israel Science Foundation at Tel Aviv University.

APPENDIX

A. THE SCALING LAWS DERIVED

The integrated X-ray luminosity and the “central” SZ parameter (in the non-relativistic case) are given by

$$L_X = 4\pi \Lambda_0 n_2^2 T_2^\epsilon R^3 \int_0^1 dx x^2 \left(\frac{n}{n_2}\right)^2 \left(\frac{T}{T_2}\right)^\epsilon \quad (\text{A1})$$

$$y_0 = \frac{2k\sigma_T}{m_e c^2} n_2 T_2 R \int_0^1 dx \frac{n}{n_2} \frac{T}{T_2},$$

where we have used averaged spherical symmetry in terms of the non-dimensional radial coordinate $x = r/R$, and have normalized the electron density n and the temperature T to their values n_2 and T_2 at $r = R$. Here the expression $\Lambda_0 T^\epsilon$ approximates the X-ray emissivity in terms of the normalization Λ_0 (taking on values around 2×10^{-27} erg cm³ s⁻¹ K^{-1/2} for bremsstrahlung emission) and of the power-law index ϵ (ranging along the cooling curve from $\epsilon \approx 1/2$ for bremsstrahlung-dominated emission to $\epsilon \approx -1/2$ for important line emissions at $kT < 2$ keV; see Sutherland & Dopita 1993).

The statistical equilibrium of the ICM within a DM potential well of depth marked by the virial temperature T_V implies the size dependence

$$T_V \propto H^2 R^2. \quad (\text{A2})$$

Here $H(z) \equiv [\Omega_M(1+z)^3 + \Omega_\Lambda]^{1/2}$ is defined in terms of the virialization redshift z , and of the present density $\Omega_M \approx 0.27$ for the non-relativistic matter (DM + baryons) and $\Omega_\Lambda \approx 0.73$ for the dark energy in the Concordance Cosmology (Bennett et al. 2003); the approximation $H(z) \propto (1+z)$ holds for $z < 1$.

Thus we obtain the scaling laws

$$L_X \propto \mathcal{S}_X H^{-3} (T_V/T_2)^{3/2} n_2^2 T_2^{\epsilon+3/2} \quad y_0 \propto \mathcal{S}_Y H^{-1} (T_V/T_2)^{1/2} n_2 T_2^{3/2}, \quad (\text{A3})$$

in terms of the two shape factors \mathcal{S}_X , \mathcal{S}_Y defined by the integrals appearing in Eqs. (A1). As to the adiabat, its levels $K_{0.1}$ at $r \approx 0.1 R$ may be written as

$$K_{0.1} \propto \mathcal{S}_K \frac{T_2}{n_2^{2/3}} \quad (\text{A4})$$

in terms of the other shape factor \mathcal{S}_K . We will see below that all factors: T_2/T_V , \mathcal{S}_X , \mathcal{S}_Y , and \mathcal{S}_K , vary only weakly from clusters to groups, and so constitute minor corrections to the explicit scaling laws above. This stems from the circumstance that the structural function $n(r)/n_2$ entering the shape factors depends weakly on T_2 from clusters to groups, as observed by Sanderson & Ponman (2003) and Pratt & Arnaud (2003). Weak dependence of $n(r)$ is also expected from all equilibrium models (as discussed in depth by Cavaliere et al. 2002b); in fact, these show a weaker and weaker dependence in passing from King (1972) to NFW gravitational potentials (due to their DM concentration rising from clusters to groups, see Navarro, Frenk, & White 1997), or from isothermal to polytropic ICM (due to a lesser density rise toward the center).

On eliminating n_2 from Eqs. (A3) and (A4) we obtain the relations

$$y_0/y_g \propto (T_V/T_2)^{-1+\epsilon/2} (L_X/L_g)^{1/2} \quad K_{0.1}/K_g \propto (T_V/T_2)^{-1-\epsilon/3} (L_X/L_g)^{-1/3}, \quad (\text{A5})$$

which for $\epsilon = 1/2$ yield Eqs. (2) and (3) of the main text. We have normalized $K_{0.1}$, y_0 and L_X to the respective gravitational scaling $K_g \propto H^{-4/3} T_V$, $y_g \propto H T_V^{3/2}$, $L_g \propto H T_V^{\epsilon+3/2}$. Recall from § 2 that these obtain on considering $T_2 \approx T_V$, and $n_2 \propto H^2$ following the DM density, in turn proportional to the background's; note that when line emission is important $\epsilon = -1/2$ and $L_g \propto T_V$ apply, as stated in § 2.

Moreover, on eliminating n_2 and the main T_2 dependence from Eqs. (A3) we find

$$K_{0.1} \propto H^{-(18-4\epsilon)/(9-6\epsilon)} y_0^{(18+4\epsilon)/(9-6\epsilon)} L_X^{-4/(3-2\epsilon)}, \quad (\text{A6})$$

which for $\epsilon = 1/2$ yields Eq. (4) of the main text; for simplicity we have omitted the slowly T -dependent prefactors. In full, these read $(T_V/T_2)^{-1+\epsilon/2} \mathcal{S}_Y \mathcal{S}_X^{-1/2}$, $(T_V/T_2)^{-1-\epsilon/3} \mathcal{S}_K \mathcal{S}_X^{1/3}$ and $(T_V/T_2)^{(9-2\epsilon)/(9-6\epsilon)} \mathcal{S}_X^{4/(3-2\epsilon)} \mathcal{S}_Y^{-(18+4\epsilon)/(9-6\epsilon)} \mathcal{S}_K$ on the r.h.s. of Eqs. (A5) and (A6), respectively.

For the purpose of illustrating the slow dependence of T_V/T_2 , \mathcal{S}_X , \mathcal{S}_Y , and \mathcal{S}_K we now assume a specific DM potential well, and detailed hydrostatic equilibrium of the ICM with a specific relation between $n(r)$ and $T(r)$. For the latter we adopt a polytropic distribution with $T(r) \propto n(r)^{\Gamma-1}$ in terms of an average, constant index $\Gamma \approx 1.1 - 1.3$; then the temperature run writes $T(r)/T_2 = 1 + (\Gamma - 1)\beta \Delta\phi(r)/\Gamma$, in terms of the potential difference $\Delta\phi(r) = [\Phi(R) - \Phi(r)]/\sigma^2$ normalized to the DM one-dimensional velocity dispersion σ . As to the DM potential $\Phi(r)$, we use the simple King form $\Phi = -9\sigma^2 \ln[(r/r_c) + (1 + r^2/r_c^2)^{1/2}] r_c/r$ with $r_c = R/12$, but similar or better results obtain on using the NFW model. The parameter $\beta \equiv \mu m_p \sigma^2 / kT_2 = T_V/T_2$ encodes the T_2 dependence of the normalized profiles; it takes on values varying in the range from 0.7 in rich clusters to 0.5 in poor groups.

In Table A1 we show our results; for simplicity $\epsilon = 1/2$ is adopted, but we add that \mathcal{S}_X changes less than 15% for $\epsilon = -1/2$ (e.g., for $\Gamma = 1.2$ the value decreases from 0.73 to 0.65 in groups with $\beta = 0.5$). To put these changes in context, recall from § 2 that in moving from rich clusters with $kT \approx 10$ keV to groups with $kT \approx 1$ keV, $L_X \propto T^3$ is observed to decrease by factors 10^2 or more, $K_{0.1} \propto T^{2/3}$ by at least a factor 5, and $y_0 \propto T^2$ is expected to decrease by 30 or more; thus the T dependencies of the shape factors in the scaling relations constitute minor corrections. Actually, even slower variations occur in the prefactors of Eqs. (A5) and (A6) as they contain combinations of shape factors whose variations tend to compensate; e.g., for $\Gamma = 1.2$ the prefactors in Eqs. (A5) vary by 0.9 and 1.5, respectively, from clusters to groups.

TABLE A1
SHAPE FACTORS, DEPENDENCE ON T_2

β	$\Gamma = 1.1$			$\Gamma = 1.2$			$\Gamma = 1.3$		
	S_X	S_Y	S_K	S_X	S_Y	S_K	S_X	S_Y	S_K
0.7.....	1.66	7.43	0.19	1.17	5.78	0.33	0.96	4.94	0.47
0.6.....	1.15	5.29	0.24	0.91	4.42	0.37	0.79	3.93	0.51
0.5.....	0.84	3.82	0.29	0.73	3.37	0.43	0.66	3.10	0.56

NOTE. — The shape factors are computed for a polytropic ICM in equilibrium within a King's DM potential well. Recall that $\beta \equiv T_V/T_2$ ranges from 0.7 to 0.5 in moving from rich clusters to poor groups.

As to sensitivity of the SZ effect to the outer wings of the ICM distribution, note the bounds to their contribution set by the observed outer decline of the temperature $T(r)$; to give an example, the contribution to y_0 from the outer range $r \gtrsim 0.2R$ comes to 15–10% when the polytropic index ranges between $\Gamma \approx 1.1–1.3$. The T -dependence from clusters to groups, the matter relevant to the scaling relations Eqs. (3)-(5), is bounded by the slow variation of the overall shape factor S_Y given in Table A1.

B. THE ABEL EQUATION

We recall that the Abel integral equation has the form

$$f(x) = \int_x^q dt \frac{F(t)}{\sqrt{t-x}}; \quad (\text{B1})$$

here $f(x)$ is a known function, q a constant (that may be large), and $F(t)$ the unknown function. To derive the latter, multiply both sides of Eq. (B1) by $(x-\xi)^{-1/2}$ and integrate over x in the interval $[\xi, q]$:

$$\int_\xi^q dx \frac{f(x)}{\sqrt{x-\xi}} = \int_\xi^q \frac{dx}{\sqrt{x-\xi}} \int_x^q dt \frac{F(t)}{\sqrt{t-x}} = \int_\xi^q dt F(t) \int_\xi^t dx \frac{1}{\sqrt{(x-\xi)(t-x)}}, \quad (\text{B2})$$

where the second equality is obtained on exchanging the integration order; the last integral is simply π . Finally, differentiate both sides of Eq. (B2) with respect to ξ to obtain

$$F(\xi) = \frac{1}{\pi} \frac{d}{d\xi} \int_q^\xi dx \frac{f(x)}{\sqrt{x-\xi}}, \quad (\text{B3})$$

which is the Abel inversion formula.

Note that on differentiating with respect to ξ (with due attention paid to the singularity of the kernel), Eq. (B3) may be recast into the alternative form

$$F(\xi) = \frac{1}{\pi} \int_q^\xi dx \frac{f'(x)}{\sqrt{x-\xi}} + \frac{1}{\pi} \frac{f(q)}{\sqrt{q-\xi}}, \quad (\text{B4})$$

where the prime denotes differentiation with respect to x . But, apart from problems with the boundary term $f(q)/\pi\sqrt{q-\xi}$, Eq. (B4) is less useful in the context of the main text since it involves differentiation of the data or of their fit, with the related uncertainties (possibly enhanced by real clumpiness in the data) as discussed in detail by Lucy (1974) and Yoshikawa & Suto (1999).

REFERENCES

- Bahcall, J.N., & Sarazin, C.L. 1977, *ApJ*, 213, L99
 Balogh, M.L., Babul, A., & Patton, D.R. 1999, *MNRAS*, 307, 463
 Bennett, C.L., et al. 2003, *ApJS*, 148, 1
 Benson, B.A., et al. 2004, *ApJ*, 617, 829
 Bertschinger, E. 1985, *ApJS*, 58, 1
 Binney, J., & Strimpe, O. 1978, *MNRAS*, 185, 473
 Birkinshaw, M. 1999, *Phys. Rev.*, 310, 97
 Birkinshaw, M. 2004, in *Clusters of Galaxies: Probes of Cosmological Structure and Galaxy Evolution*, eds. J.S. Mulchaey, A. Dressler, and A. Oemler (Cambridge: Cambridge Univ. Press), 162
 Borgani, S., et al. 2004, *MNRAS*, 348, 1078
 Bower, R.G. 1997, *MNRAS*, 288, 355
 Carlstrom, J.E., Holder, G.P., & Reese, E.D. 2002, *ARA&A*, 40, 643
 Carlstrom, J.E., & The SPT Collaboration 2003, *Highlights of Astronomy* Vol. 13, ed. O. Engvold (San Francisco: ASP), in press
 Cavaliere, A., & Fusco-Femiano, R. 1976, *A&A*, 49, 137
 Cavaliere, A. 1980, in *X-ray astronomy* (Dordrecht: D. Reidel Publishing Co.), 217
 Cavaliere, A., Menci, N., & Tozzi, P. 1999, *MNRAS*, 308, 599
 Cavaliere, A., & Menci, N. 2001, *MNRAS*, 327, 488
 Cavaliere, A., Lapi, A., & Menci, N. 2002a, *ApJ*, 581, L1
 ——— 2002b, in *ASP Conf. Series 268, Tracing Cosmic Evolution with Galaxy Clusters*, eds. S. Borgani, M. Mezzetti, and R. Valdarnini (San Francisco: ASP), 240
 Cole, S., & Kaiser, N. 1988, *MNRAS*, 233, 637
 De Grandi, S., & Molendi, S. 2002, *ApJ*, 567, 163
 Diaferio, A., et al. 2005, *MNRAS*, 356, 1477
 Dos Santos, S., & Dorè, O. 2002, *A&A*, 383, 450
 Evrard, A.E., & Henry, J.P. 1991, *ApJ*, 383, 95
 Fabian, A.C. 2004, in *AIP Conf. Ser. 703, Plasmas in the Laboratory and in the Universe: New Insights and New Challenges*, eds. G. Bertin, D. Farina, and R. Pozzoli (AIP), 337
 Fabricant, D., & Gorenstein, P. 1983, *ApJ*, 267, 535
 Goldman, I., & Rephaeli, Y. 1991, *ApJ*, 380, 344
 Grainge, K., Jones, M.E., Pooley, G., Saunders, R., Edge, A., Grainger, W.F., & Kneissl, R. 2002, *MNRAS*, 333, 318
 Holder, G.P., Mohr, J.J., Carlstrom, J.E., Evrard, A.E., & Leitch, E.M. 2000, *ApJ*, 544, 629
 Inogamov, N.A., & Sunyaev, R.A. 2003, *AstL*, 29, 791
 Jones, C., & Forman, W. 1984, *ApJ*, 276, 38
 Jones, M.E. 2002, *ASP Conf. Ser. 257, AMiBA 2001: High-z Clusters, Missing Baryons, and CMB Polarization*, eds. Lin-Wen Chen, Chung-Pei Ma, Kin-Wang Ng, and Ue-Li Pen (San Francisco: ASP), 35
 Kaiser, N. 1986, *MNRAS*, 222, 323
 Kaiser, N. 1991, *ApJ*, 383, 104
 Kim, W.-T., & Narayan, R. 2003, *ApJ*, 596, L139

- King, I.R. 1972, *ApJ*, 174, L123
- Kitayama, T., et al. 2004, *PASJ*, 56, 17
- Komatsu, E., et al. 2001, *PASJ*, 53, 57
- Kosowsky, A. 2003, *NewAR*, 47, 939
- Lamagna, L. et al. 2005, in *Background Microwave Radiation and Intracluster Cosmology*, ed. F. Melchiorri and Y. Rephaeli, in press
- Lapi, A., Cavaliere, A., & De Zotti, G. 2003, *ApJ*, 597, L93
- Lapi, A., Cavaliere, A. & Menci, N. 2005, *ApJ*, 619, 60
- Lo, K.Y. 2002, in *ASP Conf. Ser. 257, AMiBA 2001: High-z Clusters, Missing Baryons, and CMB Polarization*, eds. Lin-Wen Chen, Chung-Pei Ma, Kin-Wang Ng, and Ue-Li Pen (San Francisco: ASP), 3
- Lombardi, M., et al. 2005, *ApJ*, in press (preprint astro-ph/0501150)
- Lucy, L. B. 1974, *AJ*, 79, 745
- Mahdavi, A., Boehringer, H., Geller, M.J., & Ramella, M. 1997, *ApJ*, 483, 68
- Markevitch, M. 1998, *ApJ*, 504, 27
- Masi, S., et al. 2003, *Mem. SAIt*, 74, 96
- Mazzotta, P., Brunetti, G., Giacintucci, S., Venturi, T., & Bardelli, S. 2004a, *J. Korean Astron. Soc.*, 37, 381
- Mazzotta, P., Rasia, E., Moscardini, L., & Tormen, G. 2004b, *MNRAS*, 354, 10
- McCarthy, I.G., Babul, A., Holder, G.P., & Balogh, M.L. 2003, *ApJ*, 591, 515
- McCarthy, I.G., Balogh, M.L., Babul, A., Poole, G.B., & Horner, D.J. 2004, *ApJ*, 613, 811
- McNamara, B.R., et al. 2005, *Nature*, 433, 45
- Molendi, S., & Pizzolato, F. 2001, *ApJ*, 560, 194
- Mushotzky, R.F. 2004, in *Clusters of Galaxies: Probes of Cosmological Structure and Galaxy Evolution*, ed. J.S. Mulchaey, A. Dressler, and A. Oemler (Cambridge: Cambridge Univ. Press), 124
- Narayan, R., & Medvedev, M.V. 2001, *ApJ*, 562, L129
- Navarro, J.F., Frenk, C.S., & White, S.D.M. 1997, *ApJ*, 490, 493
- Norman, M. 2005, in *Background Microwave Radiation and Intracluster Cosmology*, ed. F. Melchiorri and Y. Rephaeli, in press
- Osmond, J.P.F., & Ponman, T.J. 2004, *MNRAS*, 350, 1511
- Peebles, P.J.E. 1993, *Principles of Physical Cosmology* (Princeton: Princeton Univ. Press)
- Piffaretti, R., Jetzer, Ph., Kaastra, J.S., & Tamura, T. 2005, *A&A*, 433, 101
- Ponman, T.J., Sanderson, A.J.R., & Finoguenov, A. 2003, *MNRAS*, 343, 331
- Pratt, G.W., & Arnaud, M., 2003, *A&A*, 408, 1
- Reese, E.D., Carlstrom, J.E., Joy, M., Mohr, J.J., Grego, L., & Holzapfel, W.L. 2002, *ApJ*, 581, 53
- Rephaeli, Y. 1995, *ARAA*, 33, 541
- Rephaeli, Y. 2005, in *Background Microwave Radiation and Intracluster Cosmology*, ed. F. Melchiorri and Y. Rephaeli, in press
- Ricker, P.M., & Sarazin, C.L. 2001, *ApJ*, 561, 621
- Roussel, H., Sadat, R., & Blanchard, A. 2000, *A&A*, 361, 429
- Sanderson, A.J.R., & Ponman, T.J. 2003, *MNRAS*, 345, 1241
- Sarazin, C.L. 1988, *X-Ray Emissions from Clusters of Galaxies* (Cambridge: Cambridge Univ. Press)
- Schmidt, R.W., Allen, S.W., & Fabian, A.C. 2004, *MNRAS*, 352, 1413
- Schwan, D., et al. 2003, *NewAR*, 47, 933
- Silk, J., & White, S.D.M. 1978, *ApJ*, 226, L103
- Sunyaev, R.A., & Zel'dovich, Ya.B. 1972, *Comm. Astroph. Sp. Sc.*, 4, 173
- Sutherland, R.S., & Dopita, M.A. 1993, *ApJS*, 88, 253
- Tozzi, P., & Norman, C. 2001, *ApJ*, 546, 63
- Valageas, P., & Silk, S. 1999, *A&A*, 350, 725
- Vikhlinin, A., Markevitch, M., Murray, S.S., Jones, C., Forman, W., & Van Speybroeck 2005, *ApJ*, in press (preprint astro-ph/0412306)
- Voit, G.M., & Bryan, G.L. 2001, *Nature*, 414, 425
- Voit, G.M., Balogh, M.L., Bower, R.G., Lacey, C.G., & Bryan, G.L. 2003, *ApJ*, 593, 272
- Woody, D.P., et al. 2004, *SPIE*, 5498, 30
- Wu, K.K.S., Fabian, A.C., & Nulsen, P.E.J. 2000, *MNRAS*, 318, 889
- Yoshikawa, K., & Suto, Y. 1999, *ApJ*, 513, 549
- Zaroubi, S., Squires, G., de Gasperis, G., Evrard, A. E., Hoffman, Y., & Silk, J. 2001, *ApJ*, 561, 600
- Zhang, T., & Wu, X. 2000, *ApJ*, 545, 141